AIAA 93-0414

Doppler Global Velocimetry Measurements of the Vortical Flow Above an F/A-18

Joseph W. Lee
James F. Meyers
NASA - Langley Research Center
Hampton, VA

Angelo A. Cavone
ViGYAN, Inc.
Hampton, VA

and

Karen E. Suzuki
George Washington University
Hampton, VA

31st Aerospace Sciences
Meeting hibit
January 11-14, 1993 / Reno, NV

Doppler Global Velocimetry Measurements of the Vortical Flow Above an F/A - 18

by

Joseph W. Lee
James F. Meyers
NASA - Langley Research Center
Hampton, Virginia 23681

Angelo A. Cavone
ViGYAN, Inc.
Hampton, Virginia 23666

and

Karen E. Suzuki
Joint Institute for the Advancement of Flight Sciences
George Washington University
Hampton, Virginia 23666

Abstract

A Doppler global velocimeter was used to investigate the vortical flow above an F/A-18 model at 25-degrees angle of attack. The measurements indicate that the flow had the same characteristics as the vortical flow above a standard delta wing. The flow pattern indicating transition from stable to burst conditions found above the delta wing was also found at the 440 station above the F/A-18. Measurements downstream at the 524 station found that the flow velocity varied considerably, with standard deviations reaching 30 percent of free stream. However, individual data images indicated that the flow was spatially coherent, and not chaotic as expected.

Nomenclature

c	Speed of light, m/sec
$\hat{i}$	Laser beam propagation direction
IVC	Iodine vapor cell
$\hat{o}$	Collected scattered light direction

V Velocity of a particle passing through the laser beam, m/sec

X Cross tunnel coordinate, m

Y Vertical coordinate, m

Z Streamwise coordinate, m

$\Delta\nu$ Doppler shift frequency, Hz

ν Laser output frequency, Hz

θ Angle between the laser propagation direction and the collected scattered light, deg

Introduction

The F/A-18 is a high performance aircraft that depends on the characteristics of the vortical flow generated by leading edge extensions to provide increased lift and enhanced maneuverability. The aircraft design was optimized through wind tunnel testing using force and moment measurements to guide the development toward the final configuration. The effects of off body flows, especially the changes in the vortical flow during normal flight maneuvers, were not recognized. When stress cracks were found at the base of the vertical stabilizers of several operational aircraft, a major research effort was begun to determine the origin of the forces causing the fatigue in the structures.

Laser light sheet visualization of the vortical flow above wind tunnel models, and photographic records of smoke traces in the vortices above the High Angle-of-attack Research Vehicle (HARV) indicated that the vortices burst at angles of attack greater than 20 degrees. These studies also indicated that the vortex path intercepted the vertical stabilizers at midspan. At 25-degree angle-of-attack, the vertical stabilizers on the HARV were observed to be in random, high amplitude oscillation. Further studies of the vortical flow were conducted in the Langley Basic Aerodynamic Research Tunnel (BART) using an orthogonal, three-component, fringe-type laser velocimeter to measure the flow above a YF-17 model (F/A-18 prototype built by Northrop) at various angles of attack, reference 1. This investigation found evidence of vortex bursting at an angle of attack of 25 degrees beginning at the 440 station and continuing downstream to intersect the vertical stabilizers at midspan. The streamwise velocity was fully reversed within the core region, with continued high speed flow rotation about the core. Standard deviations of velocity, as normalized by free stream, exceeded

30 percent in all three components. The investigation also found the flow over the outboard 60 percent of the wing to be fully separated.

While the fringe-type laser velocimeter provides nonintrusive flow diagnostics of complicated, highly turbulent flows, it requires an excessively long time to measure the velocity at a sufficient number of locations to describe the flow. The investigation in reference 1 required 8 hours of continuous tunnel running to obtain the 238 measurement points needed to describe the velocity map within the selected measurement plane. Although the flow in BART has been demonstrated to be extremely stable, 8 hours of continuous operation strains the limits of the stationary flow assumption. The development of Doppler global velocimetry provides a method that can obtain the same information in less than a second.

The Doppler Global Velocimeter

In 1964, Yeh and Cummins, reference 2, invented the Laser Doppler Velocimeter (LDV) when they used an interferometric optical system to combine Doppler-shifted, scattered laser light collected from particles passing through a laser beam with a portion of that beam. These coaxial light beams were directed to a photomultiplier where they heterodyned on the photocathode surface. The resulting output signal oscillated at the Doppler frequency. As shown in figure 1, the LDV measurement direction was the vectorial difference between the propagation direction of the collected scattered light, $\hat{o}$, and the laser beam propagation direction, $\hat{i}$. The magnitude of the Doppler shift was determined by the relationship:

$$\Delta\nu = \frac{\nu_o\,(\hat{o}-\hat{i}) \bullet V}{c} \qquad (1)$$

where $\Delta\nu$ is the Doppler shift frequency, ν is the laser frequency, V is the particle velocity, and c is the speed of light. Thus, different velocity components can be measured by using various laser propagation directions and/or locations of the receiver optical system.

In 1991, Komine, *et al*, reference 3, used the same principle to develop a new laser Doppler velocimeter. Instead of using heterodyne detection, Komine used the edge of an absorption line in Iodine vapor would act as an optical frequency discriminator, figure 2, to provide a direct measure of the Doppler frequency. Adjusting the laser frequency to the midpoint along the edge of an Iodine absorption line, collected scattered light from a stationary object in the laser beam would be attenuated 50 percent as it passed through the Iodine vapor cell. If the object were

moving through the laser beam, the scattered light would be attenuated more (or less if the direction of travel were reversed) by the Iodine vapor since the Doppler effect changed the frequency of the scattered light. The greater the velocity, the greater (or lesser) the attenuation.

Since this technique provided a direct measure of the scattered light optical frequency, it did not require the resolution of individual particles as did classic laser velocimetry. The technique only required photons of scattered light sufficient to activate the detector. It made no difference whether the scattered light originated from a solid surface, micron sized particles, or even naturally occurring 0.01 micron condensation clusters in supersonic wind tunnels. Unfortunately, the amount of collected scattered light was influenced by the number of particles within the viewed laser beam, their size distribution, and even the Gaussian intensity profile of the beam cross section. Therefore, a second detector was added to sample a portion of the collected scattered light prior to the Iodine vapor cell (IVC) to provide a reference signal. Normalization of the signal detector output by the reference detector output removed all intensity influences on the collected scattered light except the velocity dependence yielded by the Iodine vapor.

If the laser beam were fanned into a light sheet and the photodetectors were replaced by CCD arrays, a measurement system could be constructed, figure 3, that would simultaneously measure the entire velocity field within the light sheet plane. This Doppler global velocimeter (DGV), as implemented by Meyers and Komine, reference 4, produced images whose intensity magnitude at any pixel location was directly proportional to the flow velocity within the light sheet volume imaged on that pixel. Investigations of stable and burst vortices above a 75-degree delta wing by Meyers, *et al*, reference 5, illustrate the capabilities of the DGV to provide insight into the fluid mechanics of complicated flows.

Experimental Arrangement

The Basic Aerodynamic Research Tunnel (BART), reference 6, was an open circuit tunnel with a test section that measured 0.71 m high, 1.02 m wide, and 3.07 m long. The tunnel could obtain a maximum velocity of 67 m/sec in the test section with a Reynolds number of 0.43 million per meter. The air entering the tunnel was conditioned by a honeycomb structure and four antiturbulence screens prior to accelerating in an 11:1 contraction nozzle before entering the test section. The turbulence intensity was measured with a hot wire and found to be less than 0.08 percent for all flow conditions. Propylene glycol seed particles were produced by a vaporization/condensation generator

placed upstream of the honeycomb structure. The particle size distribution peaked at 0.7 microns with a skewed distribution extending to 10 microns, reference 7.

The DGV receiver optical system was located upstream, on top of the test section, viewing the top surface of the F/A-18 model, figure 4. The three velocity components were measured sequentially by routing the light sheet through the left side window, top window, and right side window in turn. The scattered light was collected using a 35 mm camera lens with a focal length adjustable from 35 to 105 mm. A 100 mm lens was placed behind the collecting lens to transfer the image to the beam splitter. The metallic beam splitter, set to 20 degrees from the optical axis to minimize polarization effects, reflected a portion of the collected scattered light to the reference camera. The remaining light was directed through the Iodine vapor cell to the signal camera.

The video images from the cameras were captured by a custom digital image processor. The processor contained a synchronization circuit which supplied the timing signal to both cameras and the two internal frame grabbers. The signal image was normalized by the reference image in real time using a table look-up method, reference 8. The original signal and reference images were transferred along with the normalized image to a microcomputer for final storage.

Data Processing

During the proof-of-concept investigation, reference 5, the normalized images obtained from the digital image processor were found to be extremely noisy, indicating further processing was necessary. The normalized images were discarded since many of the data adjustments were required on the original signal and reference images. These adjustments included pixel sensitivity normalization, low pass filtering to remove random CCD generated electronic noise, image warping to remove optical and viewing perspective distortions, and compensation for laser frequency drift.

Normal variations in pixel sensitivity were removed by using the standard technique of performing a flat field illumination of the camera at two intensity levels. The resulting images were used to determine the set of linear equations that provided the pixel sensitivity normalization. Once the sensitivities had been corrected, the acquired data image was low pass filtered by convolving it with a 3 x 3, center-weighted kernel to remove electronic noise generated during readout of the image from the CCD. For reasons described below, the two output

fields comprising the image frame were separated and treated as individual images prior to filtering.

Removal of optical and viewing perspective distortions was attempted using standard image warping techniques. While the resulting images appeared visually correct, the requirement that corresponding pixels in the two cameras must view the same volume within the light sheet was not satisfied. Thus a custom warping process was developed, reference 8, to provide the required alignment of the warped images. Unfortunately, even this approach was insufficient to yield the desired results. As part of the warping procedure, the intensity value at a pixel location in the final image was obtained by interpolation among intensities from four pixels in the original image. The problem arose because standard RS-170 cameras operate in an interlace mode. Thus, the interpolation was performed between rows of pixels that had accepted light at different times. Since the corresponding pixels in the two cameras must match not only spatially but temporally, this procedure will lead to measurement inaccuracies which appear as noise in the normalized images. If a single field were used, the interpolations would be made among data acquired simultaneously, resulting in greater measurement accuracy.

During the course of testing, the frequency of the laser output would drift, resulting in a movement of the zero velocity reference. Normally this drift would be monitored using a second Iodine vapor cell to provide the necessary zero offset for each image. Although a second cell was not available for this investigation, the zero offset could still be determined since a portion of the model illuminated by the laser light sheet was viewed by the receiver. The amplitude of a signal camera pixel viewing this area was used to monitor the laser frequency drift.

Flow Field Investigation

A previous investigation, reference 5, used the Doppler global velocimeter to measure the leading edge vortical flow above a 75-degree delta wing. The wing was set to 20.5- and 40.0-degree angles of attack to obtain stable and burst vortical flows, respectively. The results were compared with fringe-type laser velocimetry measurements obtained under the same tunnel conditions. In general, the results compared favorably. The only exception was the crossflow component comparison at 20.5-degrees angle of attack. The laser velocimeter data indicated stable vortices were present, whereas the DGV results indicated that only the left vortex matched. As shown in figure 5, the right vortex was acting as a solid body of revolution. When the angle of attack was increased to 40.0 degrees, the vortical flow pattern was a skewed solid

body of revolution with slipping edges as shown in figure 6. Knowing that the model had a 0.2-degree yaw, which caused the right vortex to burst upstream compared to the left, and the flow velocity pattern of the burst vortices, one may conclude that the pattern found in figure 5 represents the transition from stable to burst vortices. The other aerodynamic characteristic found during the investigation was the spatial coherence of burst vortices. While the range of velocity would change from image to image, the DGV results clearly indicated that a similar and repeatable pattern of velocity was present within the burst vortex. This shows that the energy contained within a stable vortex does not dissipate randomly when it bursts.

The next phase in the investigation of vortical flows, and the subject of this paper, was the examination of the flow above an F/A-18 set to 25–degrees angle of attack. The goal of this investigation was to use the global measurement capabilities of the DGV to determine if the flow above the F/A18 had similar characteristics as found above the delta wing at high angles of attack. If the burst vortices did not dissipate energy randomly, it may be possible to predict structural loading caused by vortical flows. The previous laser velocimetry measurements of the flow at the 440 and 524 stations above a YF-17, figure 7, were used to provide an estimate of the average flow pattern, figures 8 and 9, and expected velocity standard deviations, figures 10 through 12.

Since measurements using each of the three DGV components were made during different tunnel runs, the results were not combined to yield velocity measurements in the standard u, v, and w component directions. The component defined by the propagation of the light sheet from the left side of the test section, figure 13, yields the average velocity mapping shown in figure 14 for the 440 station and figure 15 for the 524 station. The image clipping on the right of the model in figures 14 and 15 was caused by model blockage of the input laser light sheet. The mirror of this component, figure 16, was obtained by propagating the light sheet through the right side. As expected, the velocity maps, figures 17 and 18, are mirrors of figures 14 and 15, respectively. The third component, figure 19, obtained by propagation of the light sheet through the top of the test section, yields the velocity maps shown in figures 20 and 21 for the 440 and 524 stations, respectively. These velocity maps indicate that the vortices are still in transition at the 440 station and fully burst at the 524 station. The characteristics of these vortices appear to duplicate the properties of the simple vortical flow found above the delta wing. There appears to be little influence on the vortices by other flows generated by aircraft structures.

Previous standard deviation amplitudes measured with the laser velocimeter were sufficient to account for loading levels that could generate the stabilizer oscillations seen in flight, provided the flow was structured. However, this data yielded little insight into the flow structure, if any, since neither temporal nor spatial correlations were possible. Laser light sheet visualization and flight video data suggested the flow was random. However, individual frames of DGV data clearly show spatially coherent structures within the burst vortices, both on the delta wing and the F/A-18. Although the velocity magnitude varies with time, the structure remains the same. Also, standard deviation maps of the flow, figures 22 through 24, are consistent with the laser velocimeter measurements.

Summary

An investigation of the vortical flow above an F/A-18 at 25-degrees angle of attack using a Doppler global velocimeter (DGV) has been presented. The capability of the DGV to simultaneously measure the velocity distribution within a selected plane provided evidence that the burst vortical flow had similar characteristics as the flow above a standard delta wing at high angles of attack. Image to image comparisons clearly show that the flow striking the vertical stabilizers was not chaotic. Flow velocity standard deviations were found to be comparable to similar results obtained above a YF-17 using a fringe-type laser velocimeter.

References

1. Sellers, W. L., III; Meyers, J. F.; and Hepner, T. E.: *LDV Surveys over a Fighter Model at Moderate to High Angles of Attack*. SAE 1988 Aerospace Technology Conference & Exposition, Anaheim, CA, October 3-6, 1988.

2. Yeh, Y.; and Cummins, H. Z.: *Localized Fluid Flow Measurements with a He-Ne Laser Spectrometer*. Applied Physics Letters, vol. 4, no. 10, pp. 176-178, May 1964.

3. Komine, H.; Brosnan, S. J.; Litton, A. B.; and Stappaerts, E. A.: *Real Time, Doppler Global Velocimetry*. AIAA 29th Aerospace Sciences Meeting, Reno, NV, paper no. AIAA-91-0337, January 7-10, 1991.

4. Meyers, J. F.; and Komine, H.: *Doppler Global Velocimetry - A New Way to Look at Velocity*. ASME 4th International Conference on

Laser Anemometry, Advances and Applications, Cleveland, OH, August 5-9, 1991.

5. Meyers, J. F.; Lee, J. W.; and Cavone, A. A.: *Three Component Doppler Global Velocimeter Measurements of the Flow Above a Delta Wing*. Sixth International Symposium on Applications of Laser Techniques to Fluid Mechanics, paper 13.2, Lisbon, Portugal, July 20-23, 1992.

6. Sellers, W. L., III; and Kjelgaard, S. O.: *The Basic Aerodynamics Research Tunnel - A Facility Dedicated to Code Validation*. AIAA 15th Aerodynamic Testing Conference, San Diego, CA, paper no. AIAA-88-1997, May 18-20, 1988.

7. Meyers, J. F.: *Generation of Particles and Seeding*. von Karman Institute for Fluid Dynamics, Lecture series 1991-08, Laser Velocimetry, Brussels, Belgium, June 10-14, 1991.

8. Meyers, J. F.: *Doppler Global Velocimetry - The Next Generation?* AIAA 17th Aerospace Ground Testing Conference, paper AIAA-92-3897, Nashville, TN, July 6-8, 1992.

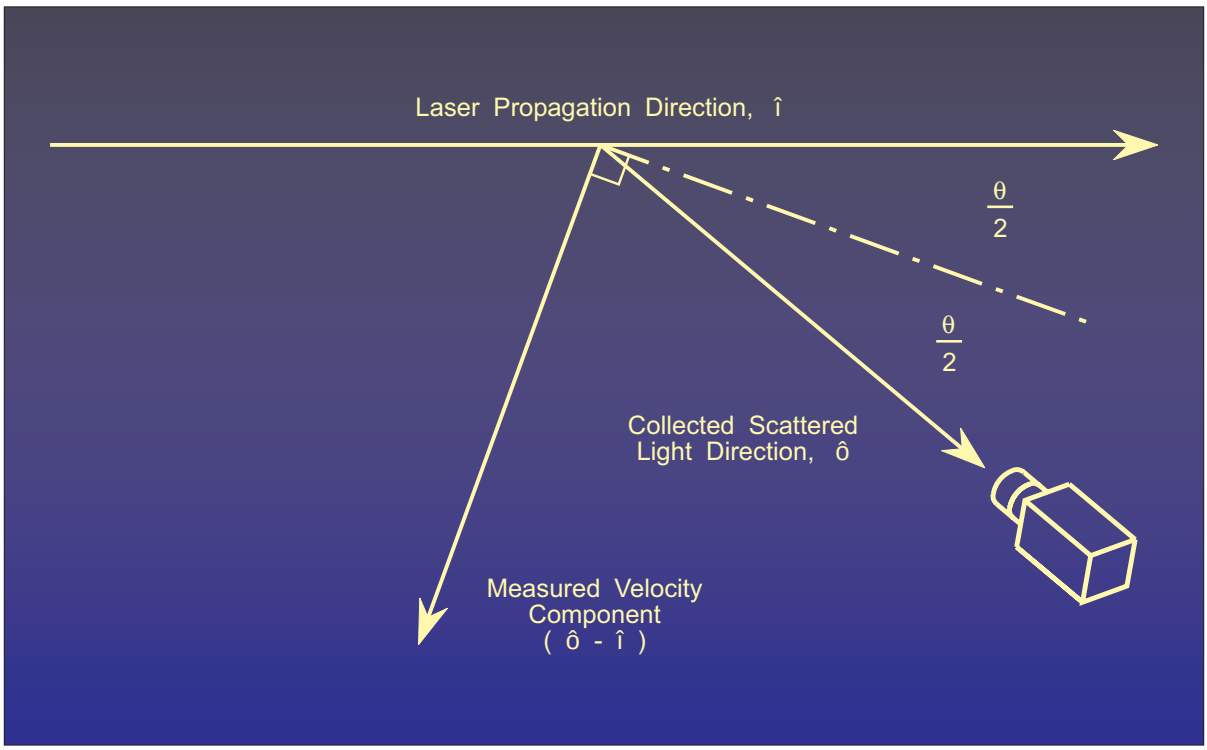

Figure 1.- Diagram depicting the velocity measurement direction based on the orientation of the laser propagation direction and the detector location.

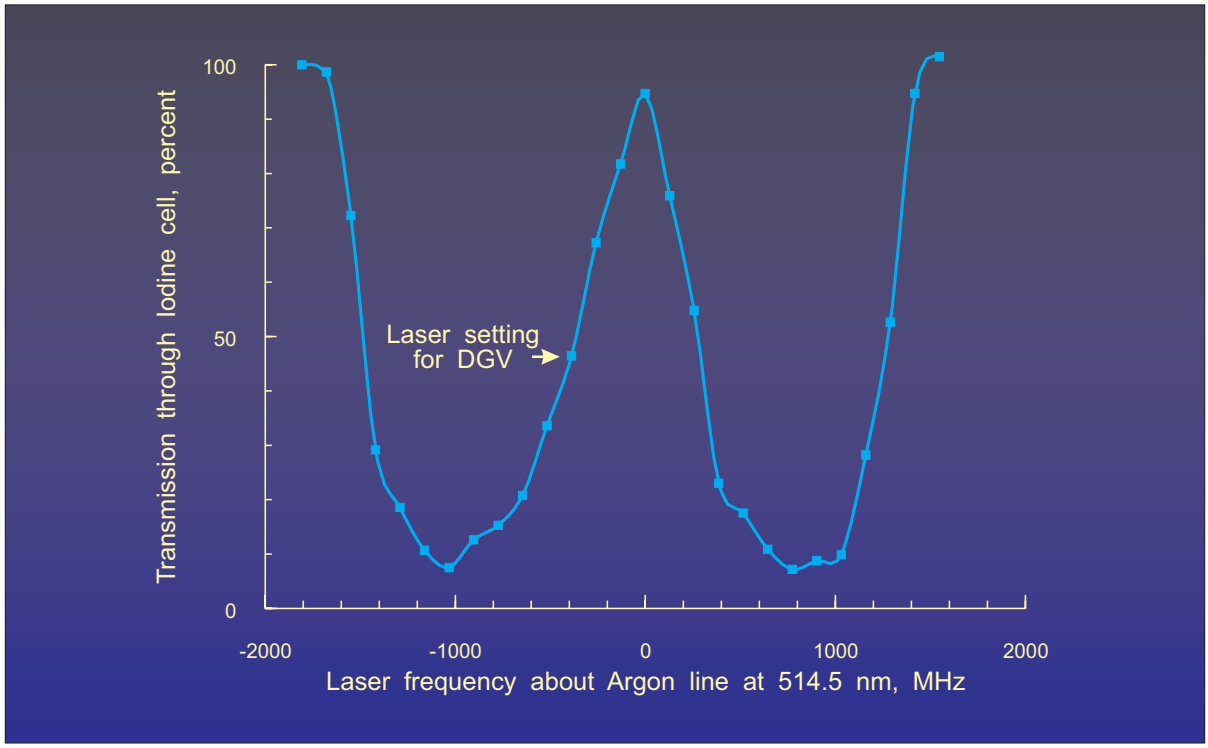

Figure 2.- Transfer function of the Iodine vapor cell, IVC.

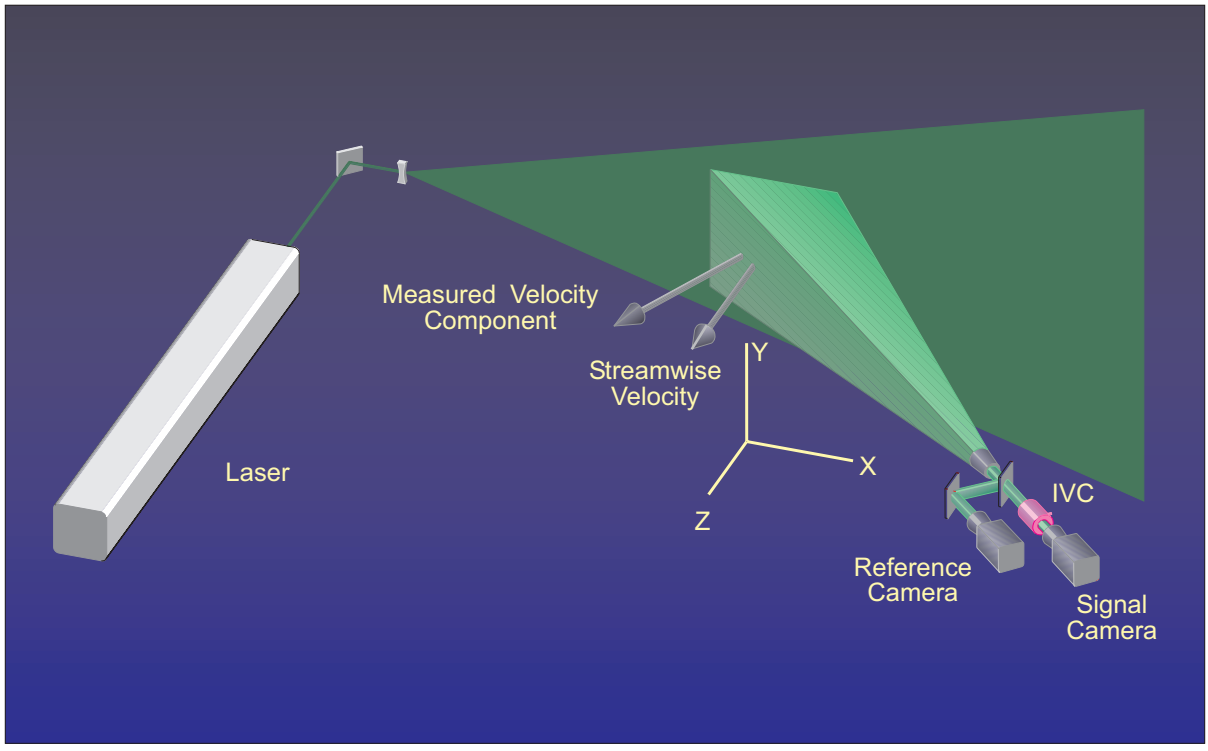

Figure 3.- Pictorial view of the Doppler global velocimeter used in the Basic Aerodynamics Research Tunnel.

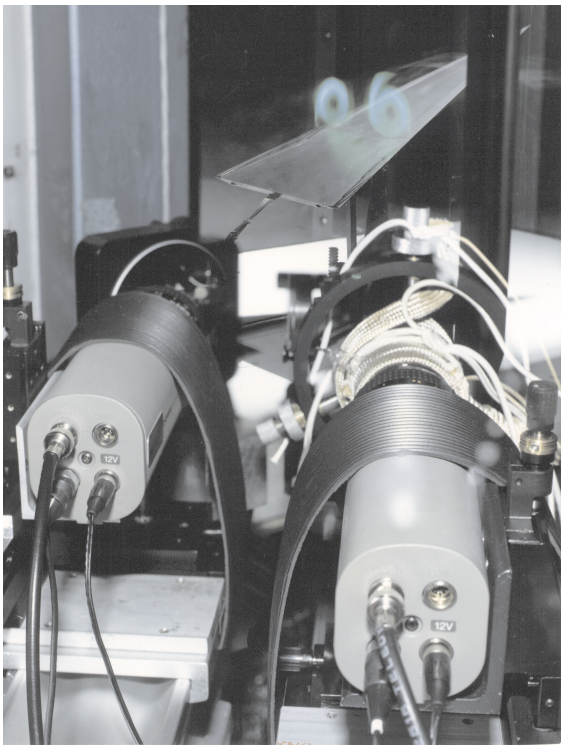

Figure 4.- Photograph of the Doppler global velocimeter installed in the Basic Aerodynamics Research Tunnel.

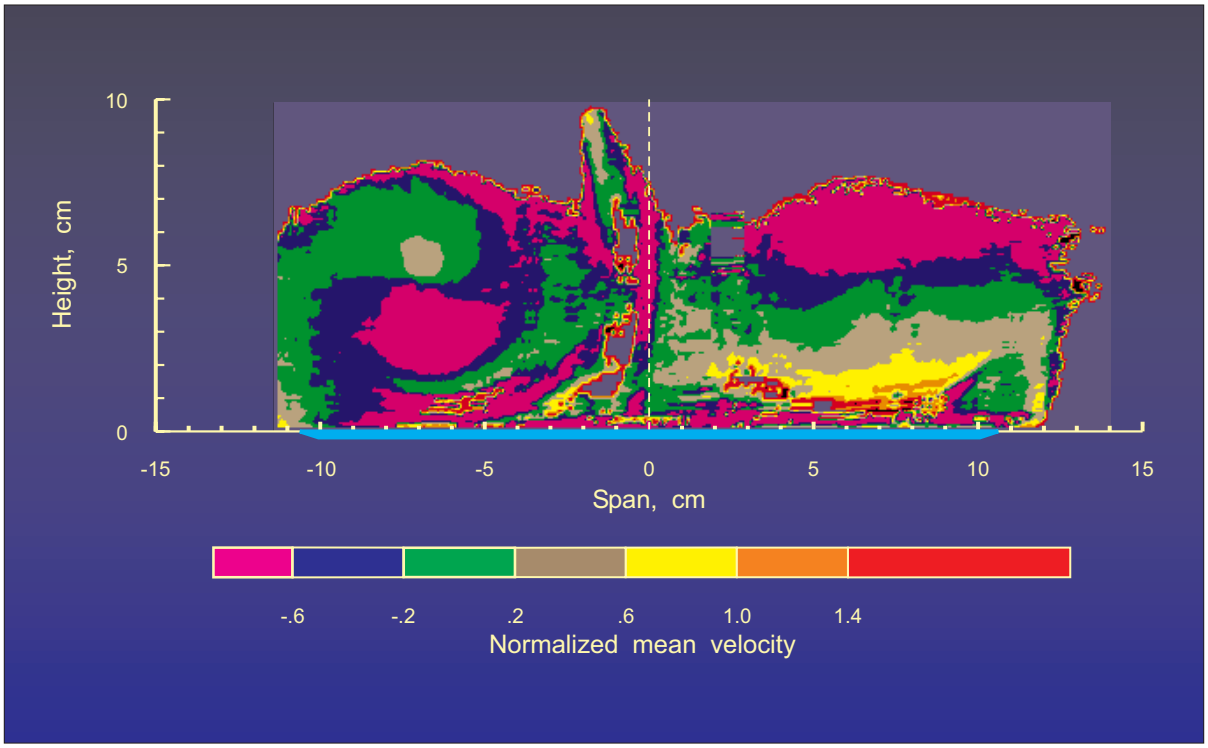

Figure 5.- DGV measurements of the cross-flow component (average of 30 frames) of the vortical flow field above a 75-degree delta wing at an angle of attack of 20.5 degrees.

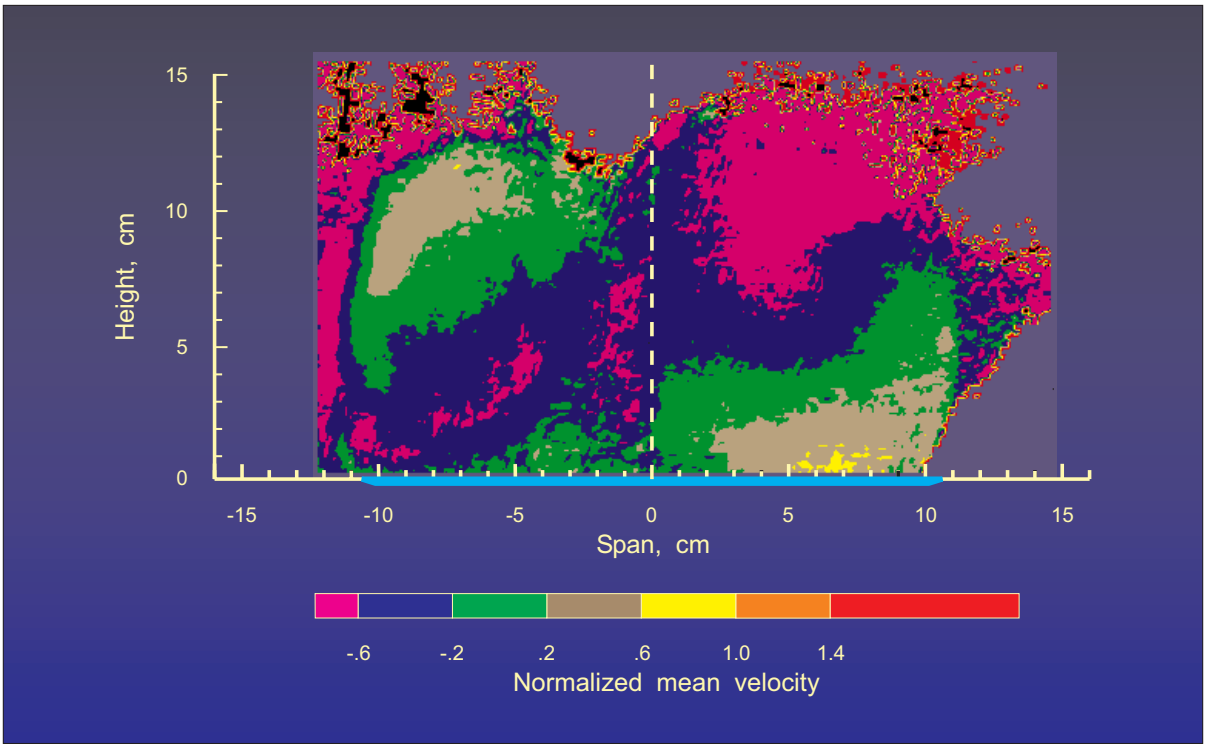

Figure 6.- DGV measurements of the cross-flow component (average of 30 frames) of the vortical flow field above a 75-degree delta wing at an angle of attack of 40.0 degrees.

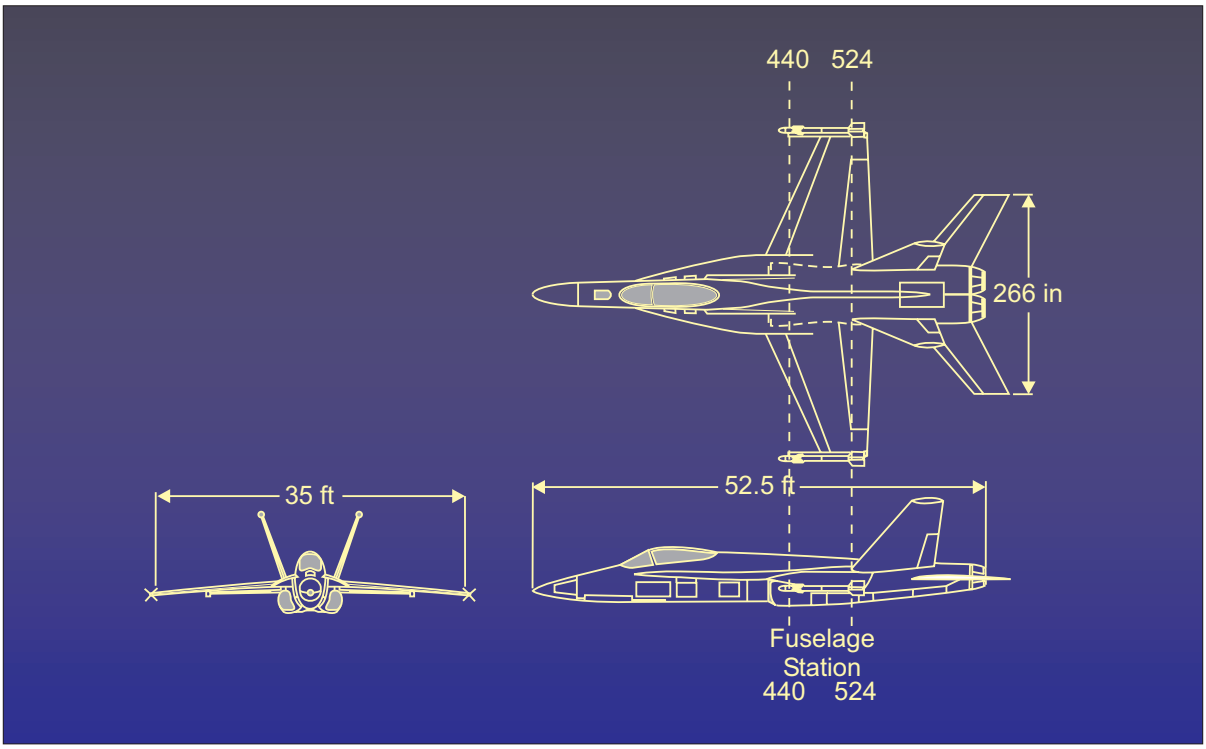

Figure 7. Three view diagram of the YF-17 configuration.

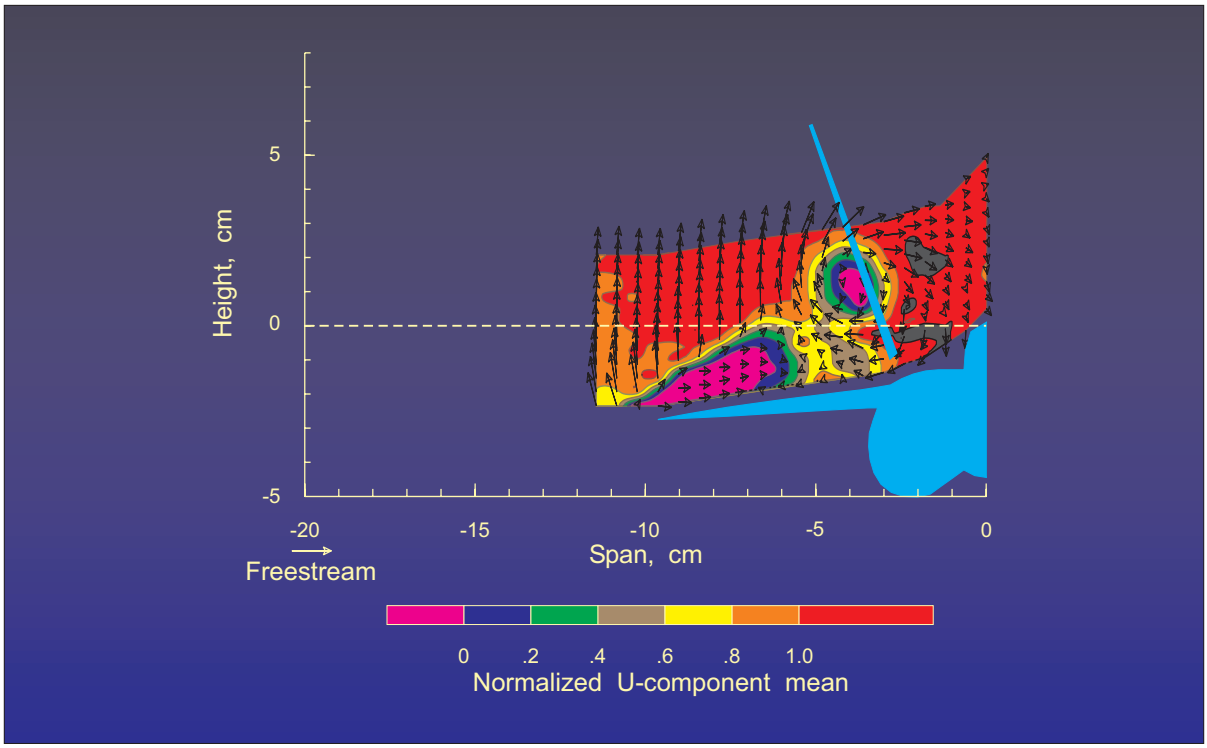

Figure 8. Mean velocity measurements of the vortex flow above the YF-17 model at an angle of attack = 25.0^{o}, station 440.

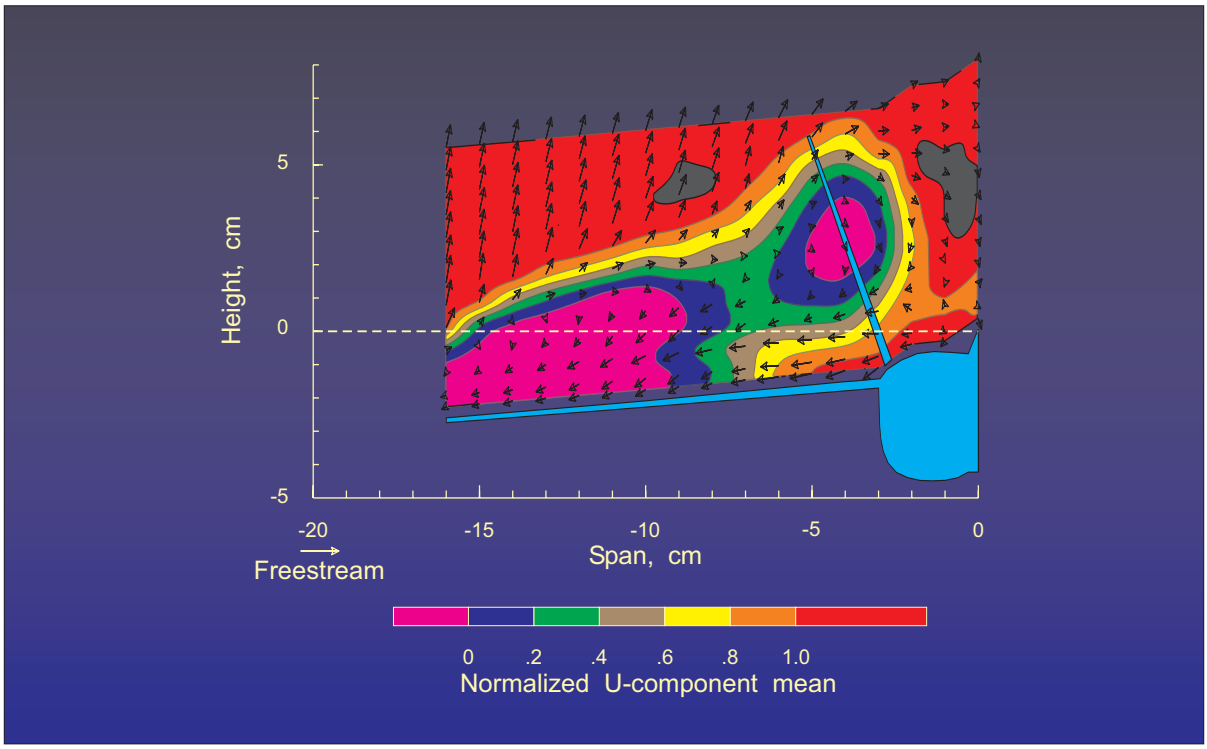

Figure 9. Mean velocity measurements of the vortex flow above the YF-17 model at an angle of attack = 25.0^{o}, station 524.

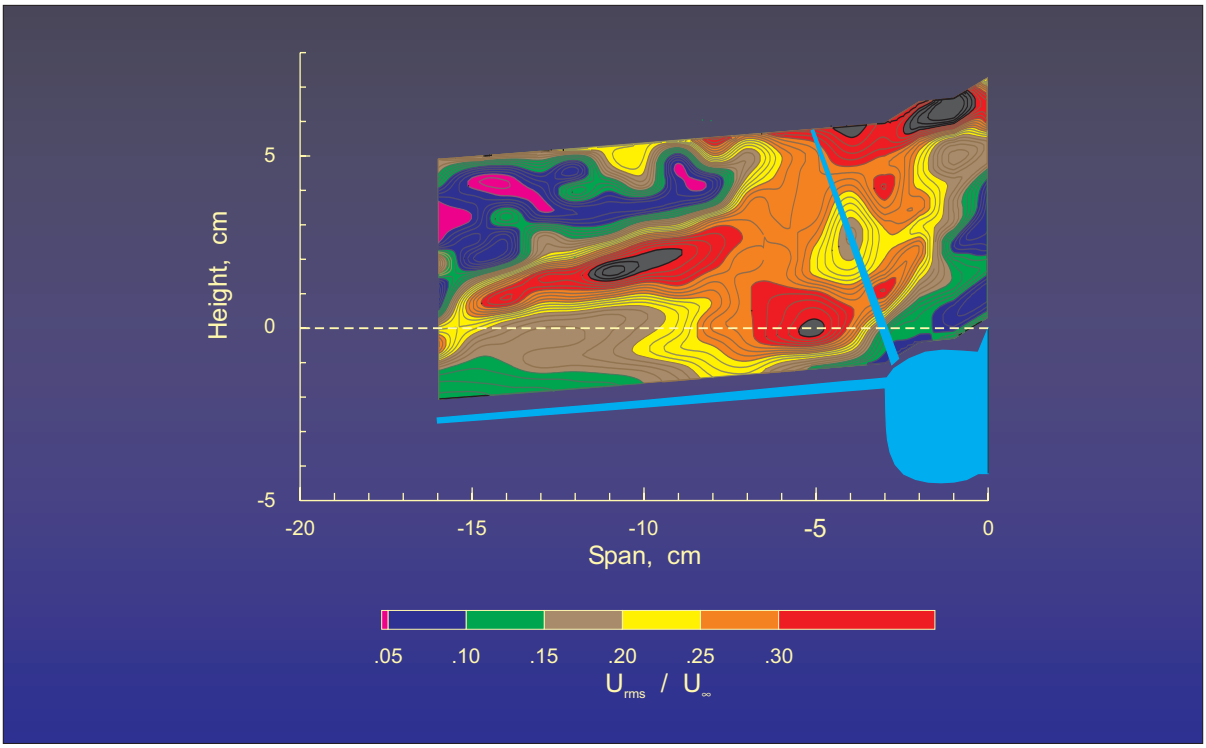

Figure 10. Contours of streamwise normalized standard deviation of the vortex flow above the YF-17 model at an angle of attack = 25.0^{0}, station 524.

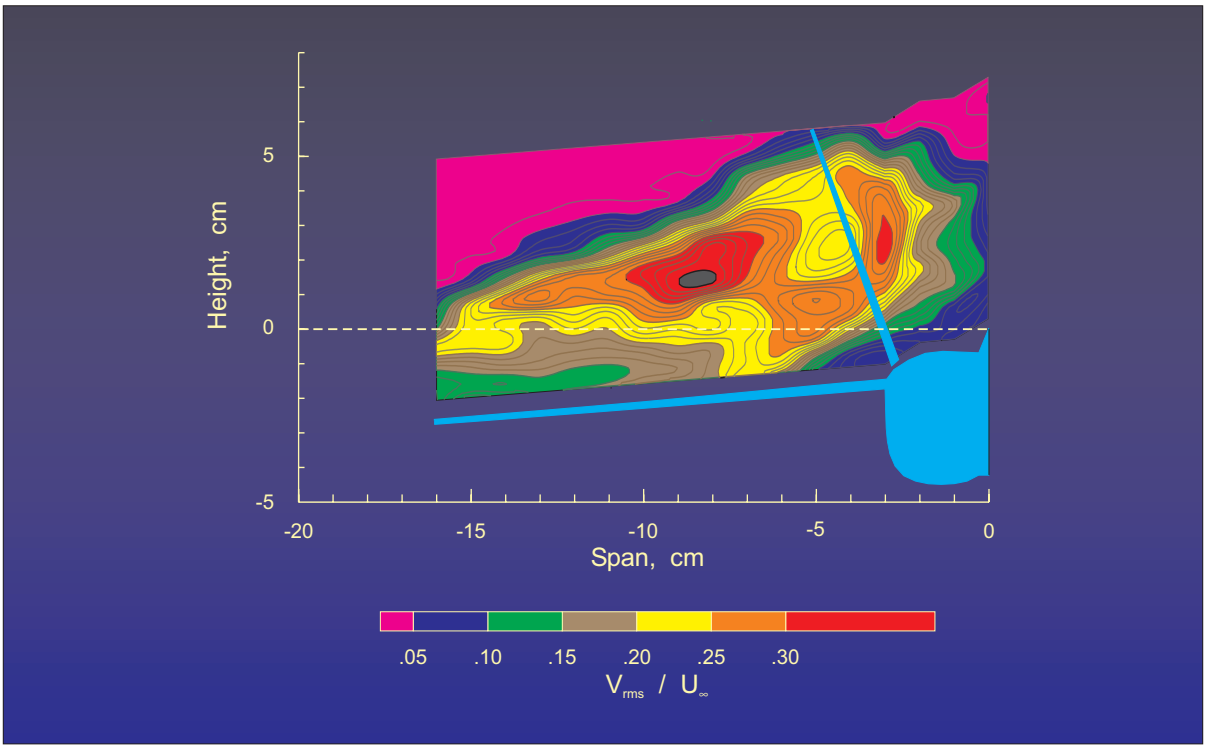

Figure 11. Contours of vertical normalized standard deviation of the vortex flow above the YF-17 model at an angle of attack = 25.0^{0}, station 524.

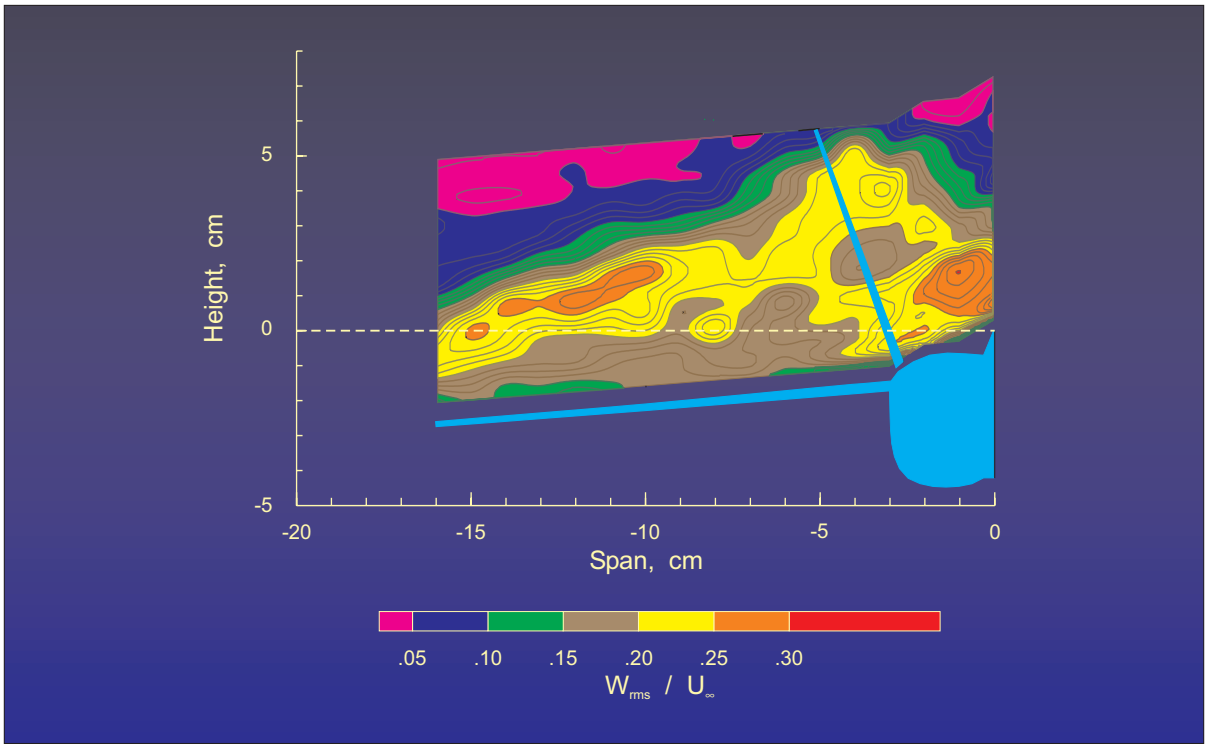

Figure 12. Contours of traverse normalized standard deviation of the vortex flow above the YF-17 model at an angle of attack = 25.0°, station 524.

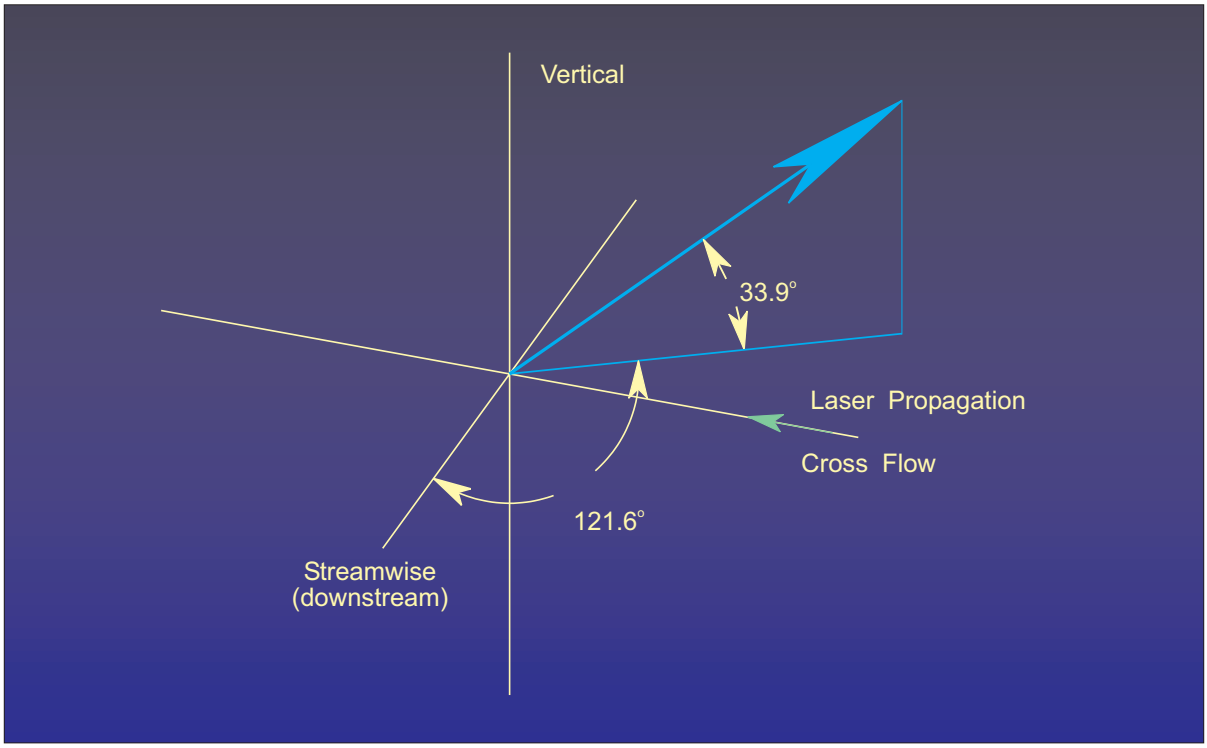

Figure 13.- DGV measurement vector with the laser propagation from the left side of the test section.

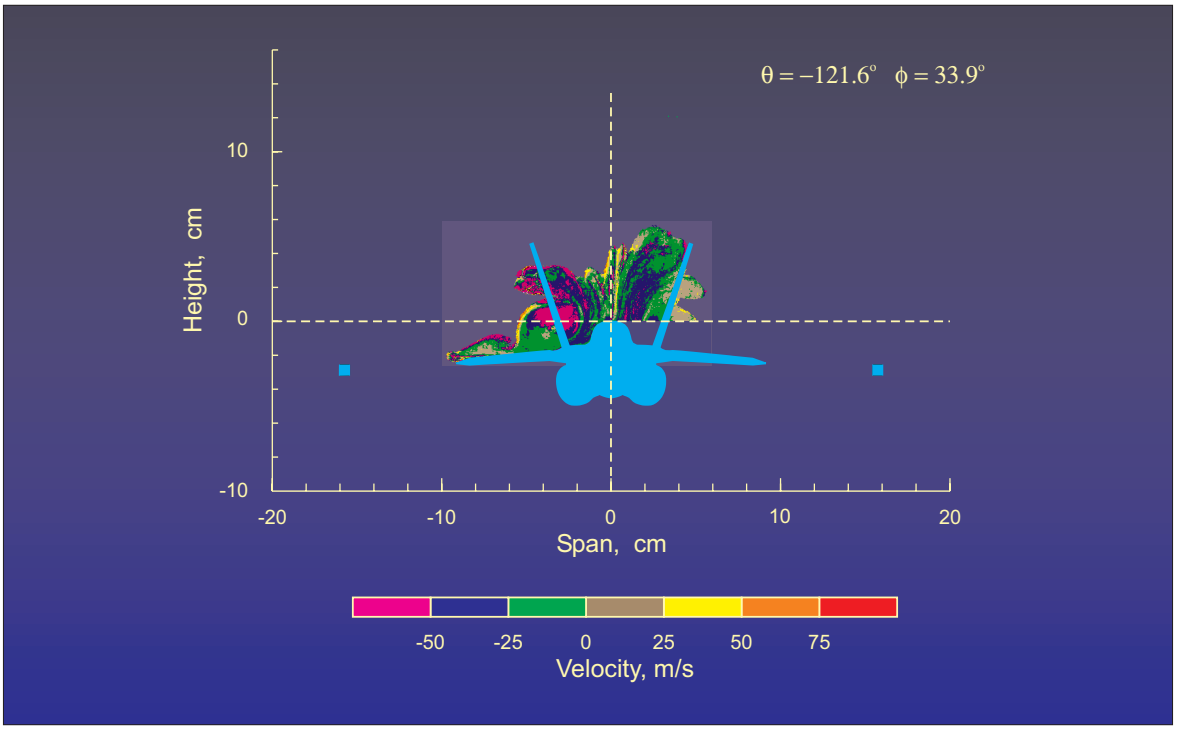

Figure 14.- DGV measurements of the velocity field (average of 30 frames) at the 440 station for the component along the direction -121.6 degrees from streamwise with an elevation of 33.9 degrees.

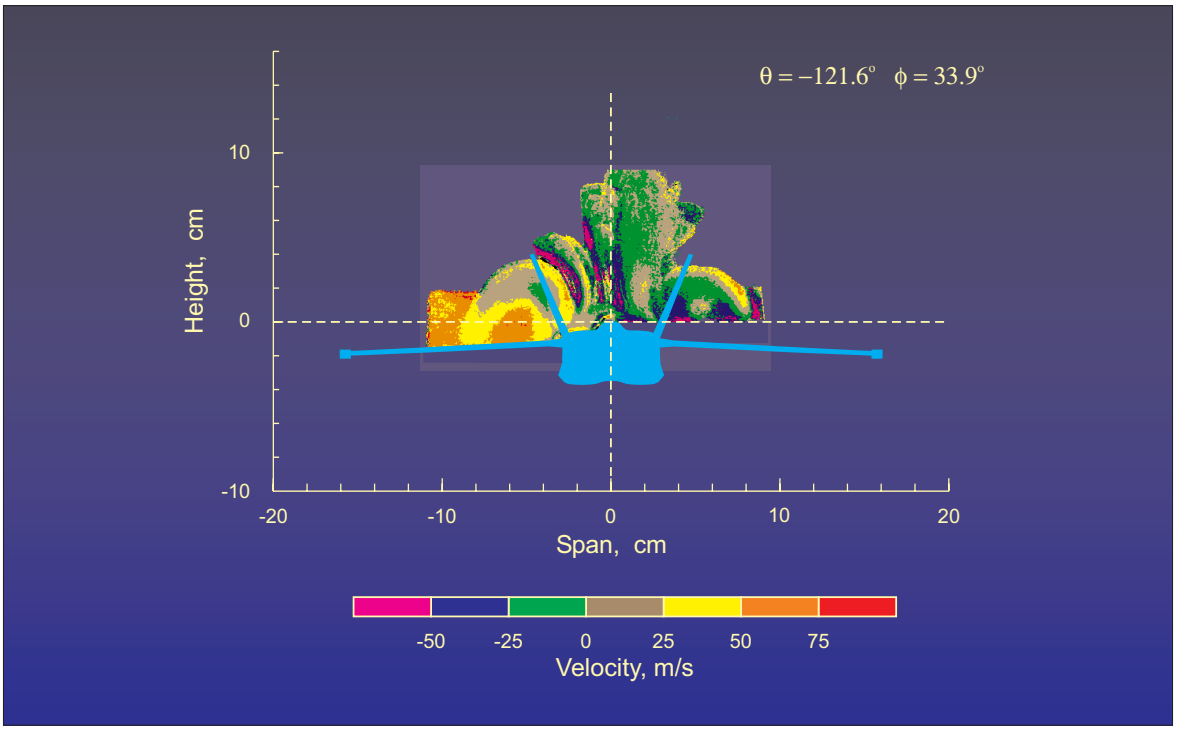

Figure 15.- DGV measurements of the velocity field (average of 30 frames) at the 524 station for the component along the direction -121.6 degrees from streamwise with an elevation of 33.9 degrees.

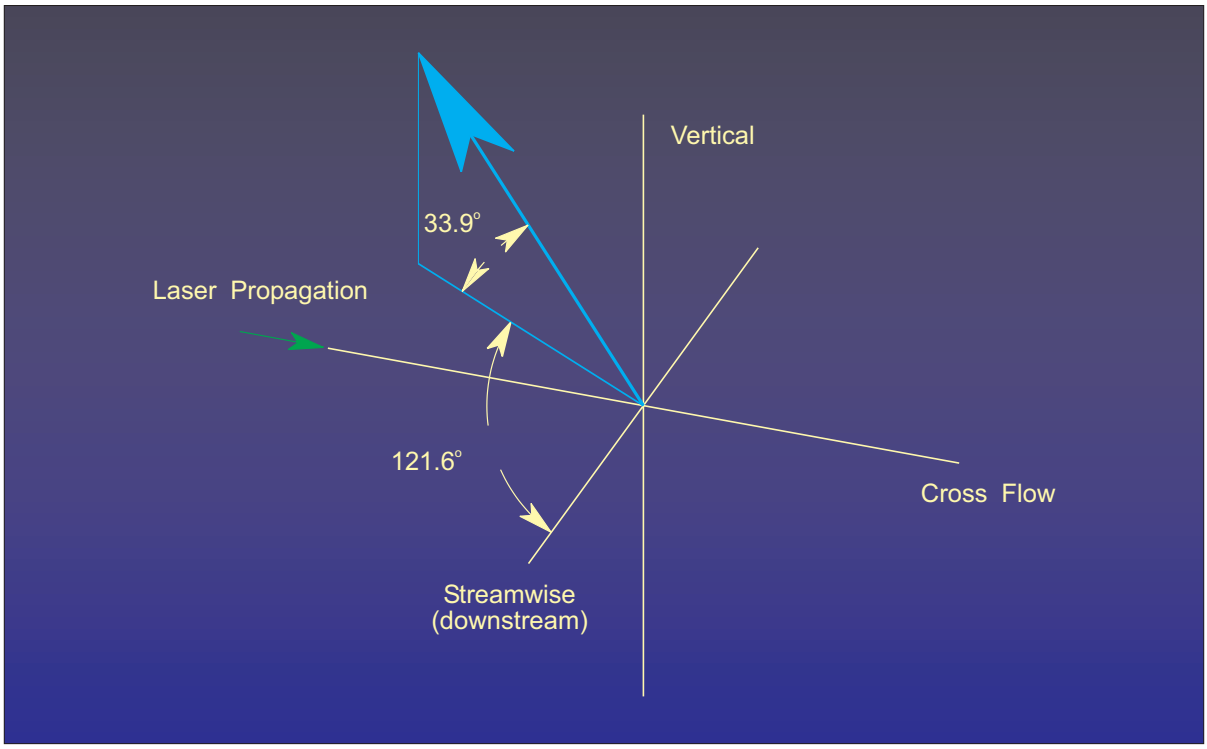

Figure 16.- DGV measurement vector with the laser propagation from the right side of the test section.

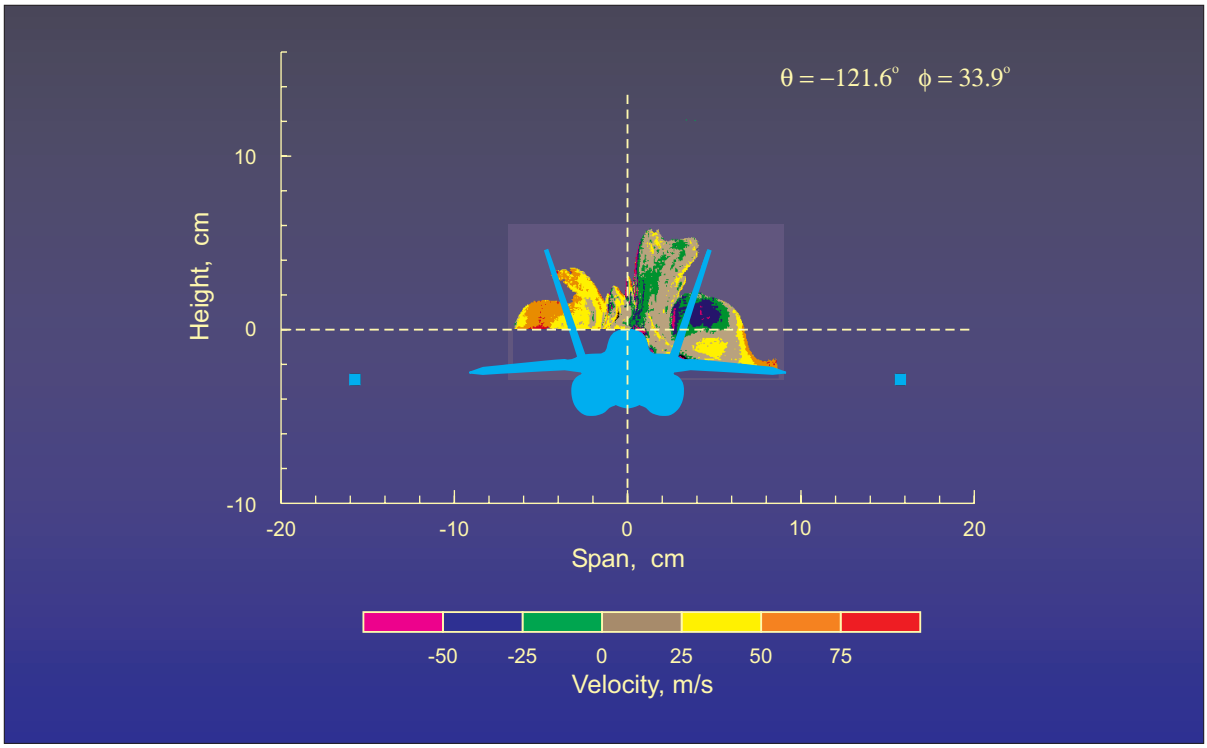

Figure 17.- DGV measurements of the velocity field (average of 10 frames) at the 440 station for the component along the direction 121.6 degrees from streamwise with an elevation of 33.9 degrees.

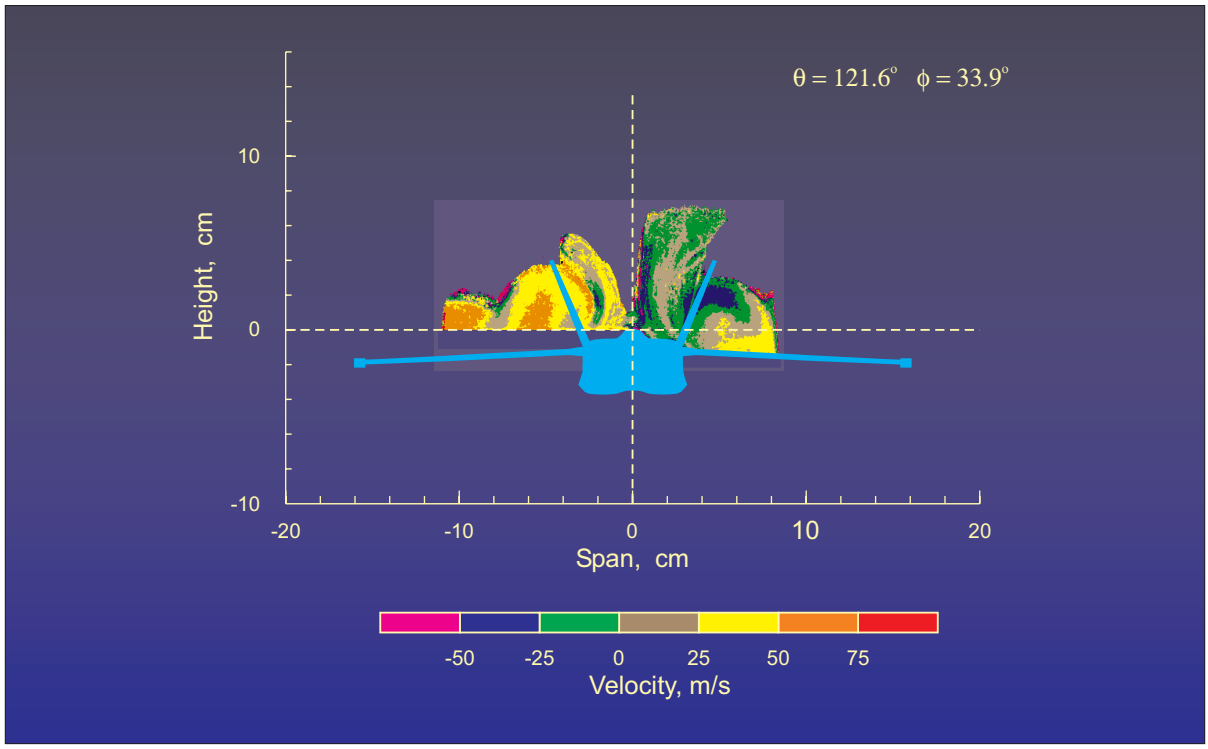

Figure 18.- DGV measurements of the velocity field (average of 30 frames) at the 524 station for the component along the direction 121.6 degrees from streamwise with an elevation of 33.9 degrees.

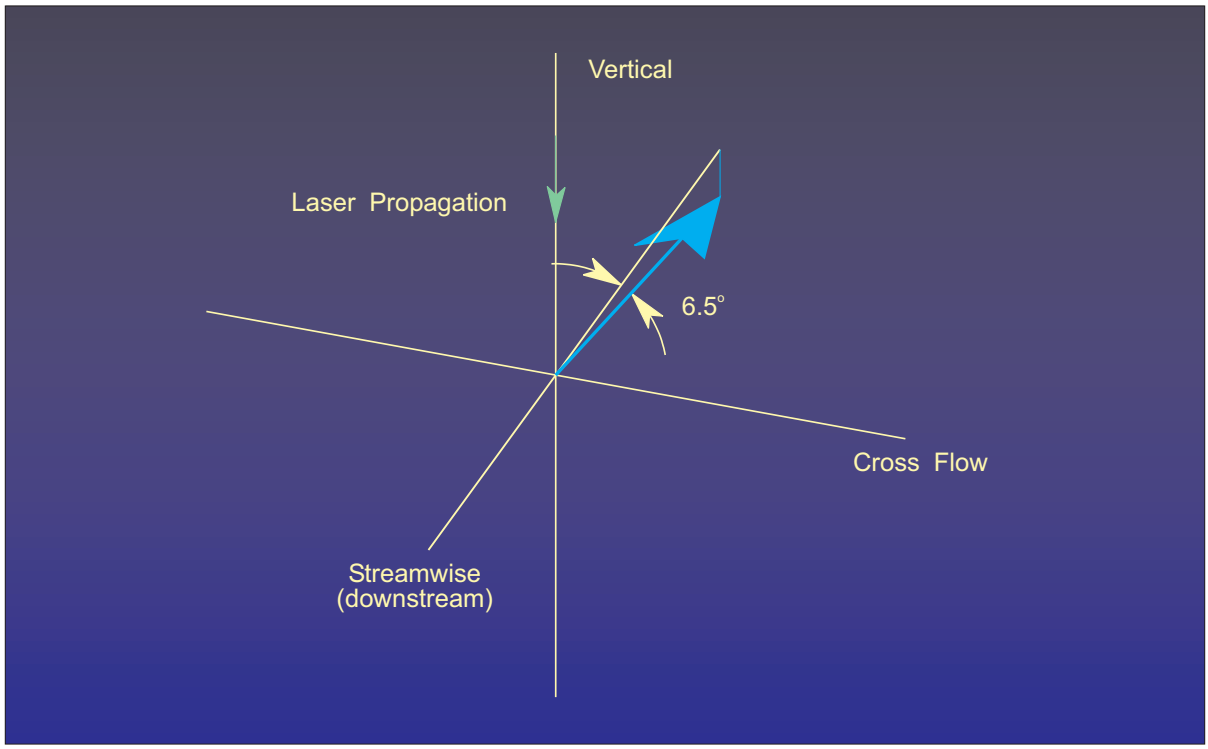

Figure 19.- DGV measurement vector with the laser propagation from the top of the test section.

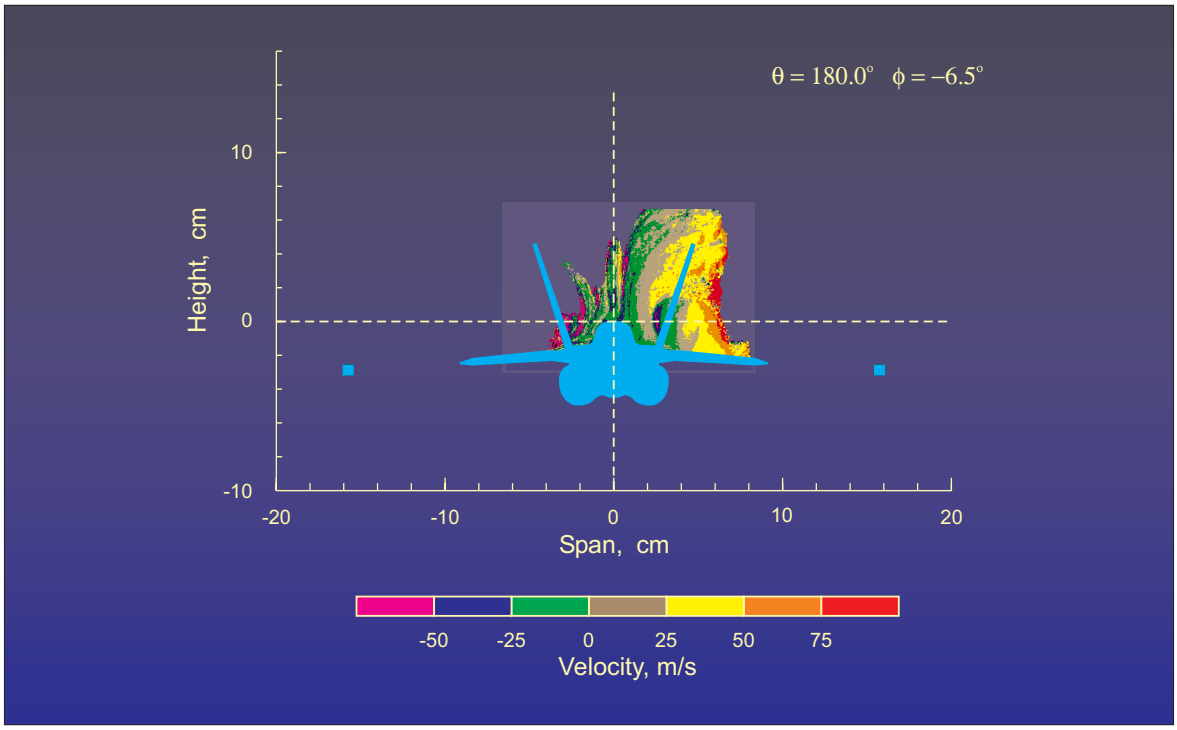

Figure 20.- DGV measurements of the velocity field (average of 30 frames) at the 440 station for the component along the direction 180.0 degrees from streamwise with an elevation of -6.5 degrees.

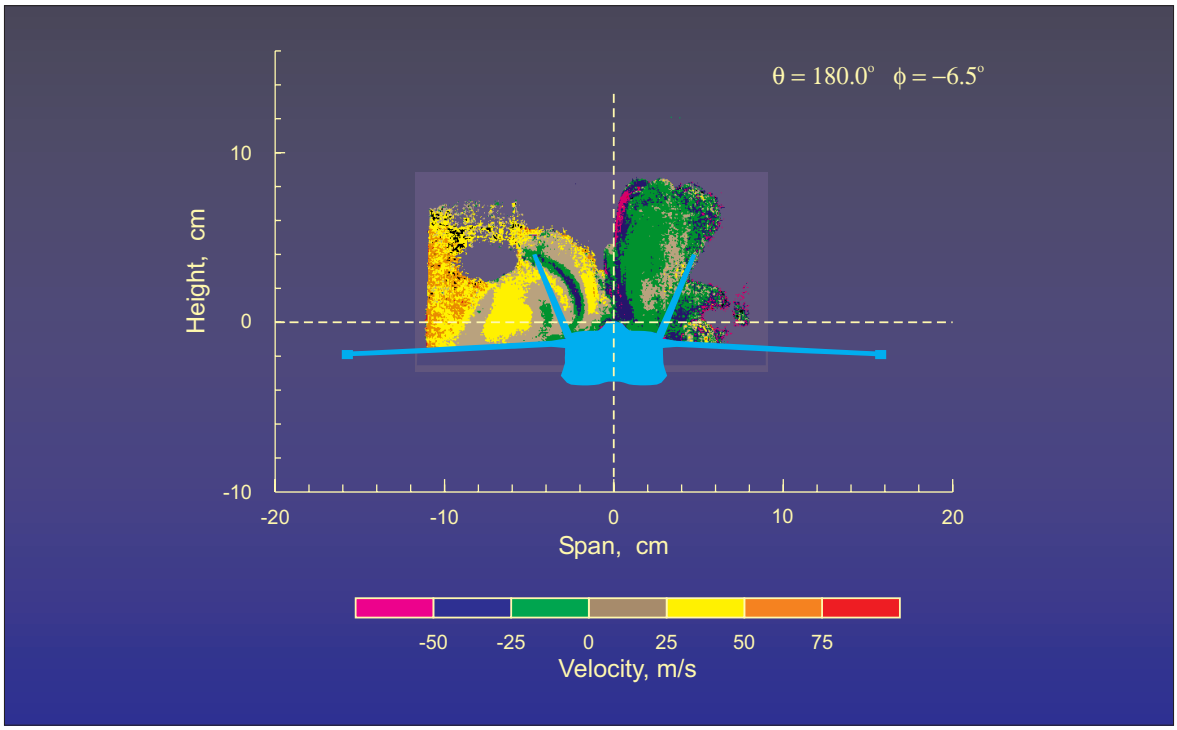

Figure 21.- DGV measurements of the velocity field (average of 30 frames) at the 524 station for the component along the direction 180.0 degrees from streamwise with an elevation of -6.5 degrees.

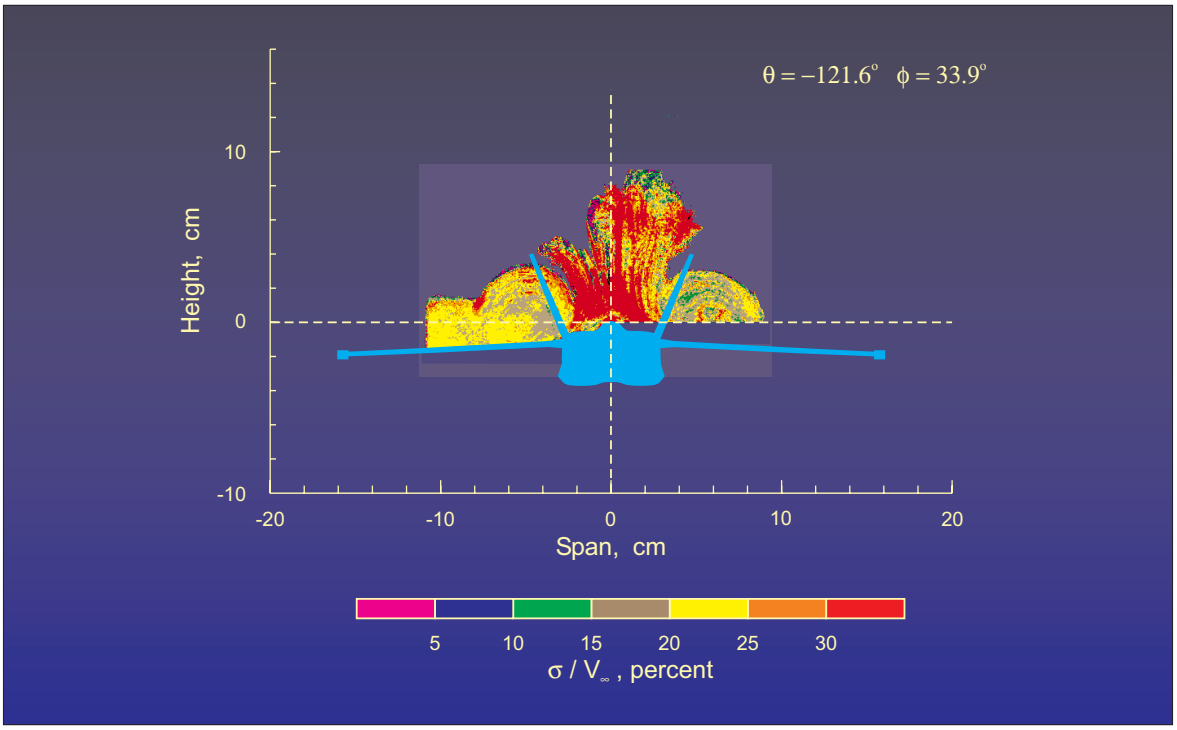

Figure 22.- Standard deviation of the velocity field, normalized by free stream, at the 524 station for the component along the direction -121.6 degrees from streamwise with an elevation of 33.9 degrees.

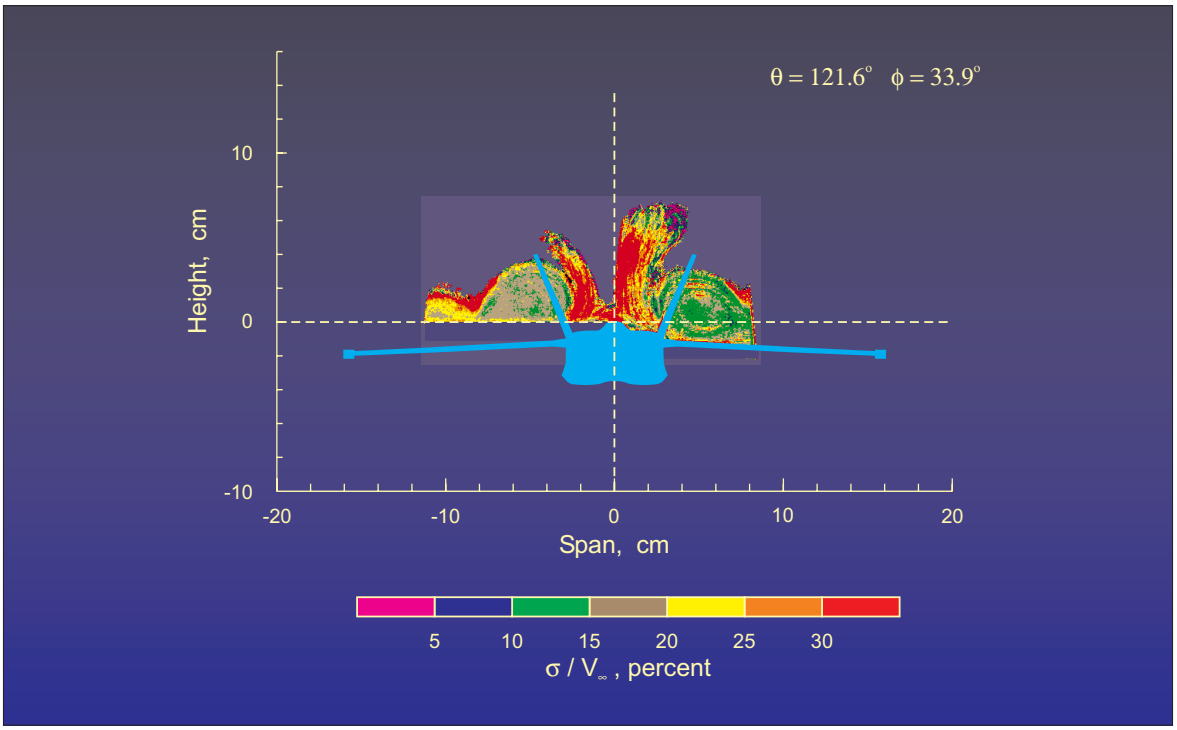

Figure 23.- Standard deviation of the velocity field, normalized by free stream, at the 524 station for the component along the direction 121.6 degrees from streamwise with an elevation of 33.9 degrees.

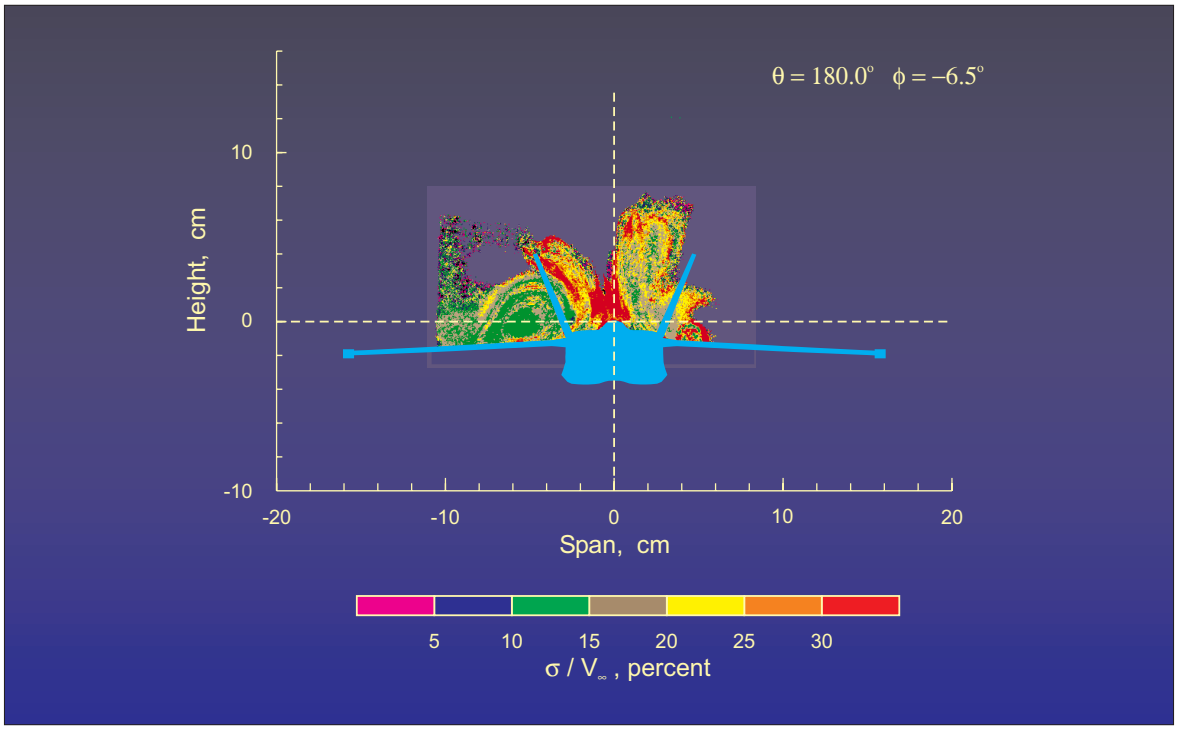

Figure 24.- Standard deviation of the velocity field, normalized by free stream, at the 524 station for the component along the direction 180.0 degrees from streamwise with an elevation of -6.5 degrees.